Mallett et al. Journal of Electric Propulsion (2025) 4:6
https://doi.org/10.1007/s44205-025-00105-5

Journal of Electric Propulsion

RESEARCH

Open Access

Development of techniques for directly measuring thrust from a superconducting applied field magnetoplasmadynamic thruster

Benjamin P. P. Mallett[1*], Celine Jane[1], Emile Webster[1] and Jens Schmidt[2]

Presented at the 38th International Electric Propulsion Conference, Toulouse, France June 23-28, 2024.

*Correspondence:
ben.mallett@vuw.ac.nz

[1] Robinson Research Institute, Victoria University of Wellington, Lower Hutt, Wellington 5010, New Zealand
[2] Institute of Aerodynamics and Flow Technology, German Aerospace Center (DLR), Göttingen, Germany

Abstract

Superconducting magnet technology can significantly improve the system-level performance of electromagnetic thrusters by reducing the size, weight and power of the magnet module. However, a superconducting magnet poses some unique challenges to accurate and direct thrust measurement, a key performance metric of any thruster. The Robinson Research Institute (Robinson) in New Zealand and the DLR Institute of Aerodynamics and Flow Technology (DLR) in Göttingen, Germany, are working together on a project to directly measure thrust from a kW-class applied-field magnetoplasmadynamic thruster (AFMPDT) with a conduction-cooled superconducting magnet for its applied field module. This paper presents results of the characterization and modification of the thrust stands at DLR and Robinson to meet the additional challenges of stray magnetic fields, cryocooler vibrations and thermal gradients associated with the superconducting magnet system. We find that after some modifications to thrust stand parts and data analysis methods, the stray magnetic field and vibrations of a cryocooler, although large at approximately 1*g* peak acceleration, should have negligible impact on accuracy of thrust measurement. Moreover, the vibrations may improve the quality of the measurement by reducing hysteresis arising from bearing stiction. A variety of methods will need to be carefully employed to reduce sensitivity to temperature, particularly to an uneven temperature distribution across the pivot axis. We deem it feasible to make direct thrust measurement in our facilities of a flight-like superconducting AFMPDT accurate to within ±3 mN for thrust up to 100 mN. The key next stage of this project involves comparative measurements of a superconducting AFMPDT planned for 2025.

Introduction

The use of superconducting magnets with electric propulsion systems, such as applied-field magnetoplasmadynamic thrusters (AFMPDTs), presents opportunities to study the relevant physics and scaling relationships [1, 2] to higher magnetic fields as well as improving the feasibility of using such thrusters on spacecraft due to a potential size, weight and power reduction of the magnet system [3]. A critical characterization of an electric propulsion system is its thrust, favoring a direct measurement to reduce uncertainty and thus improve measurement accuracy [4]. A superconducting magnet

Springer

subsystem will present several additional challenges to this already difficult task. For a superconducting magnet to operate correctly it needs to be kept at cryogenic temperatures (<80 K) and although liquid cryogens, such as liquid nitrogen, can effectively cool magnets [5, 6], we wish to build capability to measure potential space-bound systems that will need to use mechanical cryocoolers. The vibrations from such cryocoolers, combined with the stray field from a magnet operating at much higher fields than conventional AFMPDT magnets, will impact the thrust measurement apparatus.

The Robinson Research Institute (Robinson) undertakes fundamental and applied superconductivity research and has recently embarked on an AFMPDT research program [7]. The project involves an in-space demonstration of a superconducting magnet subsystem [8], and the development of a ground-based, kW-class superconducting AFMPDT [9] with applied fields of 1 T along with the establishment of ground test facilities [10]. At the DLR Institute of Aerodynamics and Flow Technology in Göttingen (DLR), electric propulsion is tested for commercial and scientific customers which includes the development of electric propulsion diagnostics as well as thrusters. Test facilities include multiple thrust stands [11, 12], one of these stands is an inverted double-pendulum based on a set of quartz glass rods, which has been used to measure different thrusters [13].

This paper relates to a collaborative project between Robinson and DLR to develop direct, accurate thrust measurement capability of superconducting AFMPDT. The project will also cross-validate measurement systems at our respective facilities and quantify the impact of vacuum-chamber size and background pressure. The project culminates in thrust measurements throughout 2025 of the full AFMPDT system at both Robinson and DLR facilities across a range of operating parameters. The paper describes initial results from characterization and modification of the thrust stands at DLR and Robinson to meet the additional challenges of associated with a superconducting AFMPDT. We take the approach of quantifying individually the impact of stray magnetic fields, vibrations and thermal gradients ahead of the integration of a complete AFMPDT system. This approach allows rapid testing of mitigation strategies with smaller subsystems, with the thruster development proceeding in parallel.

Thrust stands at DLR and Robinson

A thrust stand, see Fig. 1a, has recently been designed and built at Robinson to support its AFMPDT research program. It is a simple hanging pendulum that is currently operated in a free-swinging configuration. The pendulum pivots over a set of full-ceramic ball bearings. Motion of the pendulum is measured by an optical displacement sensor. A set of calibrated weights, that can be loaded and unloaded *in-situ* inside the vacuum chamber, is used to relate the measured displacement to force. The platform of the thrust stand, onto which the thruster is mounted, is a black-anodized aluminium optical breadboard. A custom made chiller plate is attached to the bottom of the platform and which supports a flow of approximately 2 L.min^{-1} coolant water. Details of the design and performance of the thrust stand, and accompanying test facilities, will soon be presented in a separate paper [10].

DLR-Göttingen has multiple thrust stands, but this project uses the DEPB thrust stand as described in Ref. [12, 13] and shown in Fig. 1b. It is an inverted double-pendulum

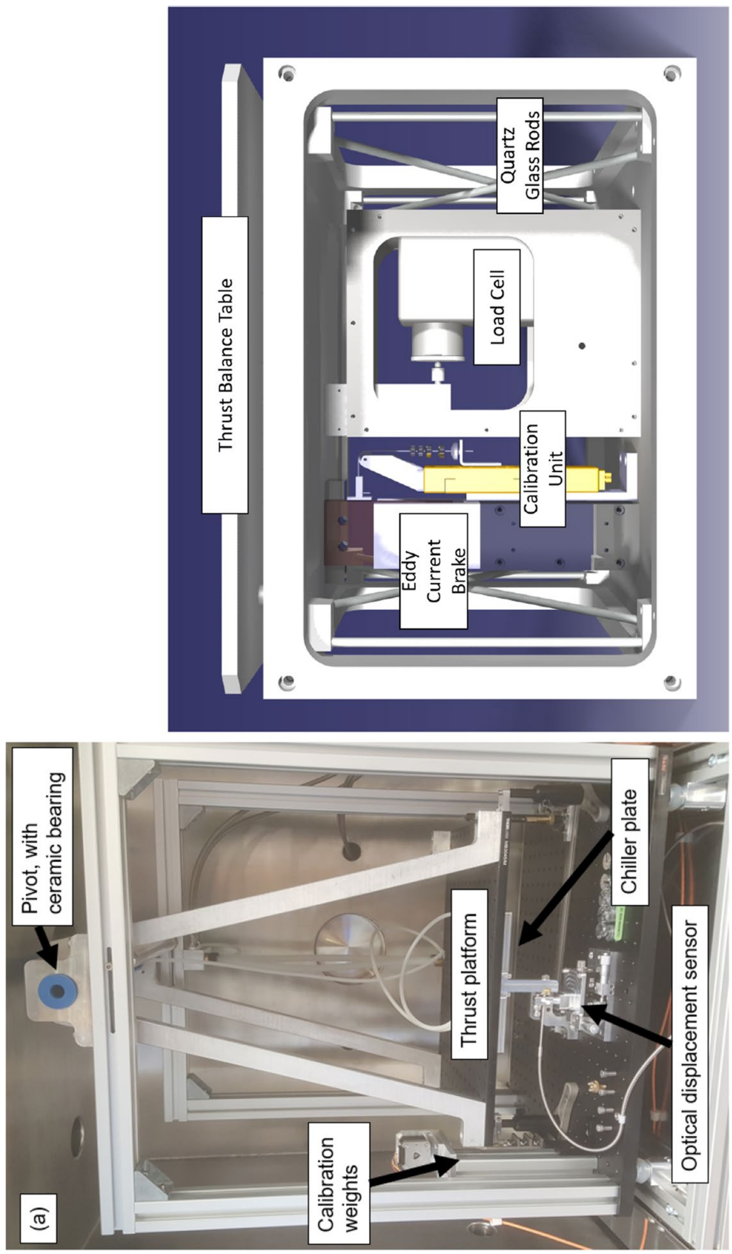

Fig. 1 **a** The thrust stand at Robinson. **b** The DEPB thrust stand at DLR (shown here as a render without side cover to better highlight its various components)

that uses a set of quartz glass rods as flexure bearings. Force is measured by a commercial Sartorius WZA224-N load-cell and is calibrated against a set of weights that can be loaded and unloaded *in-situ*. An eddy current break, comprising of a sheet of copper in between two permanent magnets, is installed to dampen oscillations of the stand.

Results

Magnetic field

Figure 2a shows the calculated magnitude of the radial stray magnet field for two indicative operational points of the superconducting magnet; a 0.3 T central field (blue curve) and a 1 T central field (green and orange curves). Vertical dashed red lines indicate the inner and outer radii of the magnet. This magnetic field, which is essentially a DC-field, could have a noticeable impact on thrust measurements by exerting a force on magnetically susceptible, e.g. strongly paramagnetic or ferromagnetic, components of the thrust stand [14]. Examples in our case include steel components (such as bolts), the load-cell or electric motors used as part of the force calibration systems.

The magnitude of the stray field expected at critical components of the thrust stands was determined to be up to 50 mT for our AFMPDT operating at 1 T. Nd-Fe-B permanent magnets were fully characterized and then used to simulate the stray field at those components of the thrust stand at DLR and Robinson. By using permanent magnets, we could test the sensitivity of individual components on the thrust stands more easily. On the other hand, using a superconducting magnet would have introduced significant heat flux and vibrations from its cryocooler, and a conventional magnet would have been impractically large, heavy and require significant power to operate.

Several magnetically susceptible components were found on the thrust stands that impacted the force measurement when subjected to the magnetic field. We replaced as many of these sensitive parts as possible with aluminium parts, for example the micrometer screw used to tension the load-cell on the DLR thrust stand. Figure 2b shows an annotated image of a magnetic field sensitivity experiment at DLR. Panel (c) of the Figure shows force calibration measurements as a function of the orientation and proximity of the permanent magnet to the micrometer after its magnetic parts had been replaced. The data show relatively minor changes in thrust stand behavior, even at the maximum field of 150 mT and 35 mT (for the two field directions respectively) shown in the figure. Similar results were found on the thrust stand at Robinson, whereby the locally-applied magnetic field caused an offset to the thrust measurement, but did not distort the scale and so could be corrected for with *in-situ* calibration.

These encouraging results will be checked with the full superconducting magnet operating on the thrust stands, however, the more significant impact of the magnet will be the vibrations and heat flux from the cryocooler that is used to cool the superconducting magnet.

Cryocooler vibrations

A CryoTel CT mechanical cryocooler from SunPower is operated in various orientations on the thrust stands and fitted with an accelerometer to monitor the exported vibrations, as shown in the simplified drawing of Fig. 3a. The drawing highlights the relative size and positioning of the cryocooler on the free-swinging thrust platform, which can

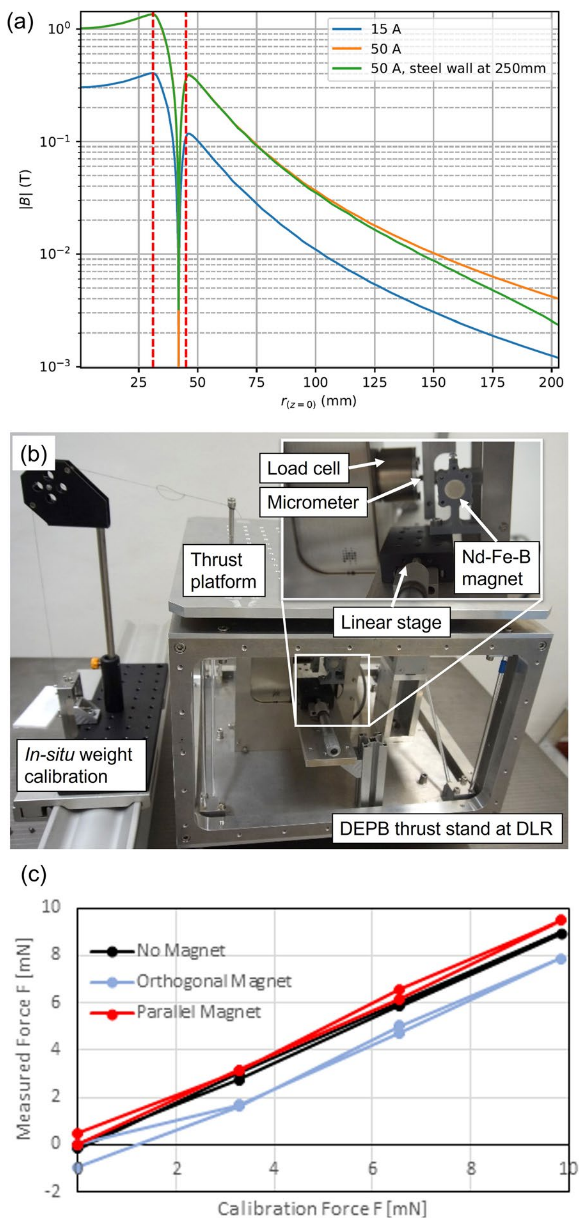

Fig. 2 **a** magnitude of the calculated stray field in the radial direction from the superconducting magnet at two operating points. **b** Annotated image of the magnetic field sensitivity tests at DLR. **c** After modifications to the thrust stands, the stray magnetic field will have only minor impact on thrust measurements. Results shown for its impact on the DLR thrust stand. See text for details

be seen in the centre of the image of Fig. 1a. The 3.1 kg cryocooler, capable of cooling the AFMPDT's superconducting magnet to its operational temperature, is powered by up to 180 W. This power ultimately ends up as heat flux that in these experiments was sunk to the thrust stand via a thermal strap. The experimental setup was essentially the same for the experiment at DLR on the DEPB thrust stand, except that the cryocooler hot-end was water cooled, with the water coolant hose freely hanging onto the thrust stand. Duplicate compact high-power loudspeakers that mimic the vibrations of the cryocooler have also been developed for comparative testing at both Robinson and DLR facilities,

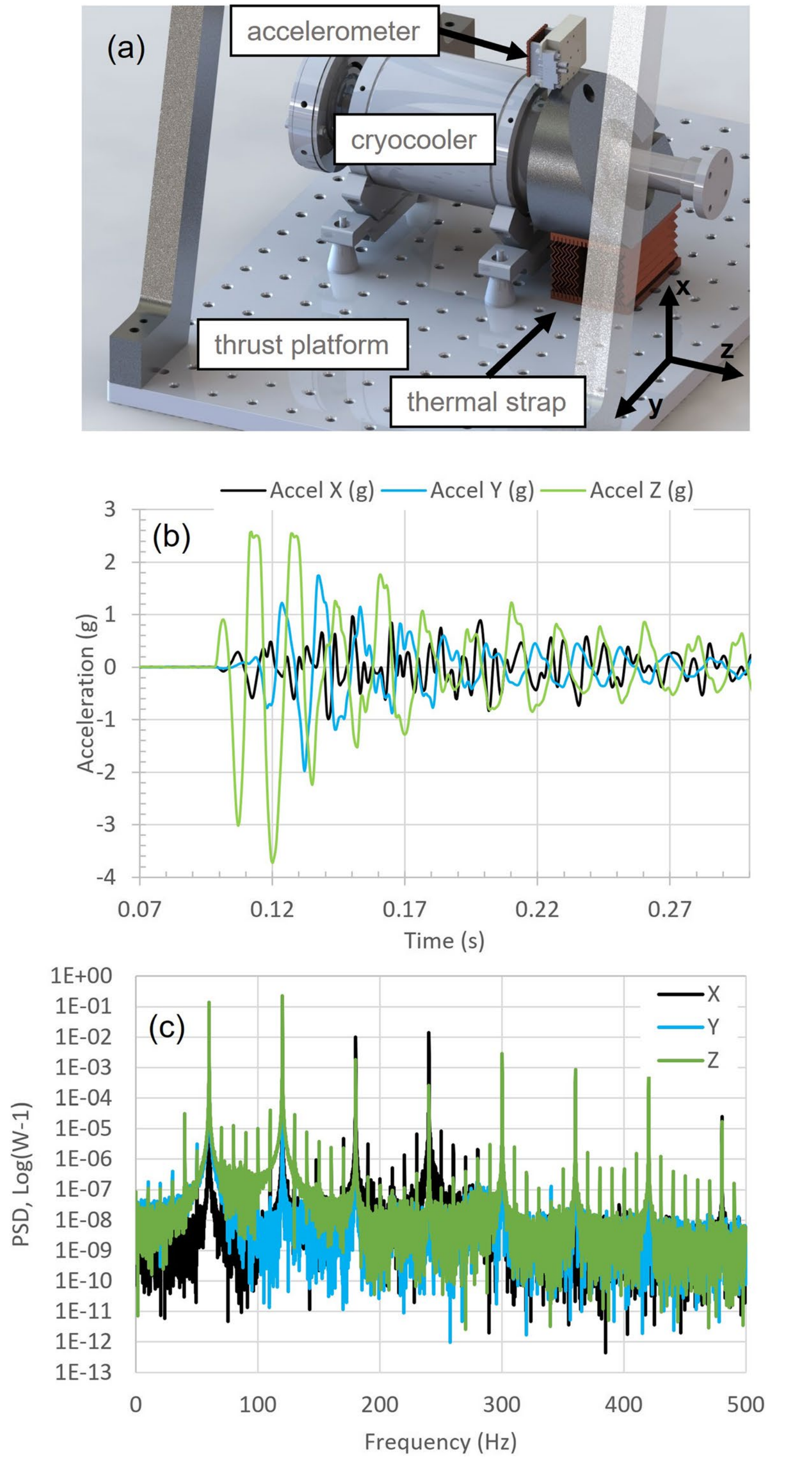

Fig. 3 **a** An illustration of the cryocooler experimental setup on Robinson thrust stand. **b** Acceleration vs time during the start-up, at 0.1 s, of the cryocooler used to cool the superconducting magnet on the AFMPDT. **c** Power spectrum of the vibrations from the cryocooler in steady state operation at 140 W

and whose frequency can be swept to experimentally identify resonances of the thrust stand.

Figures 3 and 4 show results from operating the cryocooler on the thrust stands at Robinson and DLR. Vibrations from the cryocooler have an amplitude of 1.5g (14.7 m.s^{-2}) at steady state in the axis of the cryocooler's motor (denoted the Z-axis in this case), and 0.3g in the orthogonal axes. During start up of the cryocooler however, the acceleration can exceed 3g as shown in Fig. 3b and we found it necessary to stabilize the calibration setup to avoid some of the weights being knocked out of their holders. The vibrations peak at the 60 Hz driving frequency of the cryocooler's motor and its harmonics, as shown in Fig. 3c.

Figure 4a shows the impact of these vibrations on the measurement of a set of calibration weights at Robinson. In this case, the cryocooler's motor is orthogonal to the thrust-direction of the thrust stand. The vibrations cause the oscillations in the raw data when loading a weight, which are damped over several seconds. Nevertheless, filtering of the raw data allows measurements accurate to less than 1 mN, as shown by hysteresis and a standard deviation lower than that value. Similarly, although an initial offset and significant oscillations appear in the raw data from DLR's thrust stand, shown in Fig. 4b, simple filtering of the data allows meaningful measurements to still be made. We are mindful that with loading of the thrust stand with the AFMPDT, we may shift a vibrational resonance of assembly into the cryocooler's frequency bands. In this case, we can take active measures to dampen or shift that resonance.

An unintended, and somewhat positive, consequence of the vibrations is to lessen the severity of stiction at the bearings. We believe stiction to be the leading cause of hysteresis in weight calibration measurements (a difference between the force/displacement measured whilst loading compared with unloading of the calibration weights that cannot be accounted for by baseline drift), and with the cryocooler operational hysteresis in the weight calibration measurements is effectively removed.

These preliminary results also show that temperature change on the thrust stand caused by the cryocooler have as big an impact as the vibrations themselves. For example, note the baseline drift in the raw data of Fig. 4a that became prominent once the heat generated by the cryocooler's was sunk to the thrust stand platform. Experimental studies to quantify and mitigate these thermal effects are explored further in the following section.

Thermal effects

We have undertaken investigations into the temperature sensitivity of the thrust stands. The superconducting AFMPDT will have two main sources of heat flux into the system, up to 180 W from the cryocooler and potentially up to a few kilo-Watts from the thruster. In principle, the associated temperature variation can impact the thrust measurement via; materials properties (e.g. stiffness of flexure bearings or cables), sensitivity of sensors, and structural distortions that lead to a change in the centre-of-mass (CoM) on the stand. Ahead of integrated thruster testing, we have therefore undertaken a series of experiments seeking to assess and better understand the thermal sensitivity of the devices at DLR and Robinson.

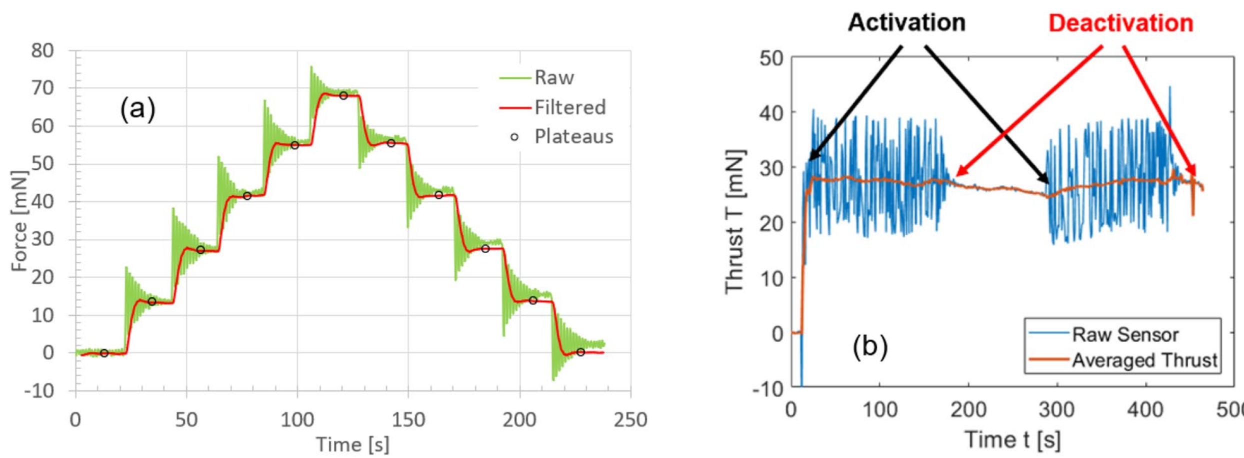

Fig. 4 **a** Loading then unloading calibration weights on the thrust stand at Robinson with the cryocooler operating at 60 W input power. **b** Operating the cryocooler on the thrust stand at DLR

To study the thermal sensitivity independently, multiple electrical heaters and temperature sensors are mounted on the thrust stands and operated to produce temperature variations and gradients. Calibration-weight and cold-gas thruster measurements are used to assess the impact on the force measurement. For the tests on the DLR thrust stand, four 12.5 W heaters were placed in the corners of the stand's moving platform and Pt100 temperature sensors placed either end of the platform, and on the fixed base of the stand. The passive thermal insulation between the platform and its instrumentation below on the fixed base was removed, to maximize the sensitivity to temperature of the platform. Sample data from these experiments are shown in Fig. 5, with a schematic of the experiment layout shown in the inset.

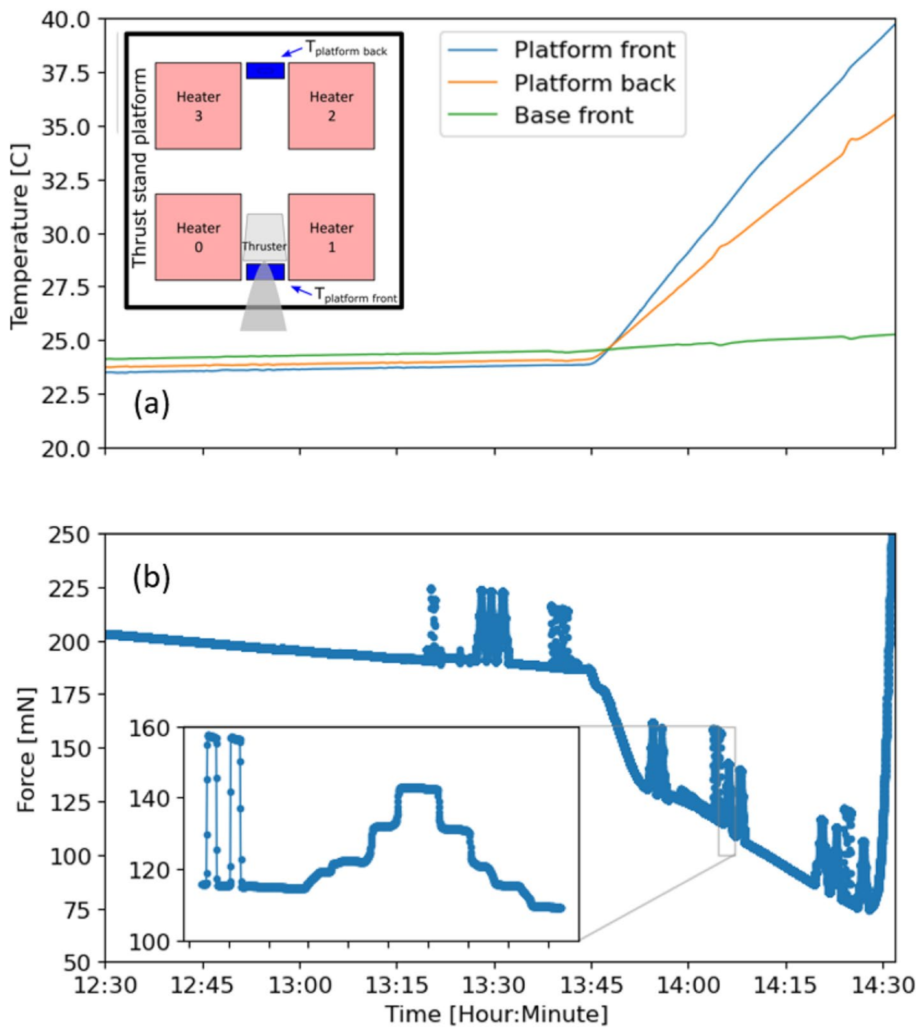

Fig. 5 Temperature sensitivity studies of the thrust stand at DLR. Panel **a** shows temperatures measured at two locations on the movable platform, and one location on the fixed base of the thrust stand. The inset shows a top-down schematic view of the experiment layout, with locations of the heaters as pink squares, the cold-gas thruster, and the two temperatures sensors on the movable platform as blue rectangles. Panel **b** shows the load-cell reading over the same time period. Gold-gas thruster and calibration weight measurements are run intermittently, as highlighted by the inset

The temperature of the vacuum chamber used in this experiment is not actively stabilized, and so varies over the course of a day. That temperature variation is observed on the thrust stand also, as approximately 0.5 $K.hr^{-1}$ in this case. Concurrently, the output of the load-cell monotonically drifts at a rate of approximately -18 $mN.hr^{-1}$. Combining these results gives a sensitivity of -36 $mN.K^{-1}$, although we note that doing so might imply the drift in the load-cell is caused by the temperature change.

Once the heaters are powered up to 50 W, at 13:45 in Fig. 5, the temperature variation of the thrust stand increases to 24 $K.hr^{-1}$, and there is a rapid variation in the baseline of the load-cell output also. However, the interspersed calibration-weights and cold gas thruster measurements, one of which is highlighted in the inset to Fig. 5b, returned consistent force measurements before and after activation of the heaters, once the variation in the baseline had been accounted for. This encouraging result means accurate thrust measurements can still be made outside of thermal stability of the thrust stand.

Despite the rapid variation in the baseline load-cell reading due to actively heating the thrust stand, when expressed as a temperature sensitivity at -9 $mN.K^{-1}$, it is significantly lower than the unforced temperature variation case discussed above. This suggests that none of the monitored temperatures are the relevant ones, if indeed a single temperature is the relevant variable. For example, it may be that the spatial temperature distribution is more significant as it shifts the centre-of-mass on the thrust stand. We have started to investigate these hypotheses further in subsequent studies on the thrust stand at Robinson.

A similar set of experiments were undertaken at Robinson. It is not our intention to directly compare thermal-drift performance, as might be captured by the $\Delta F/\Delta T$ metric used above. The experiments at DLR were testing a 'worst-case' scenario whereby there was no active and minimal passive (e.g. multi-layer insulation) temperature control, on an inverted pendulum thrust stand. On the other hand, the thrust stand at Robinson is operated as a simple, free-swinging pendulum that is actively water-cooled and which therefore will be less sensitive to heat loads. Rather, these studies seek investigate the cause of thermal sensitivity, its mitigation and assess its potential impact on the measurement of our kW-class thruster.

Figure 6 shows a selection of results from these temperature sensitivity studies at Robinson. In the top row of the Figure, a 90 W heater is located in the centre of the thrust stand and turned on intermittently, as indicated by bars along the time-axes. Panel (a) shows the temperature measured either side of the pivot axis, as indicated by the inset schematic. In this case, both temperatures at 'C1' and 'D1' show an approximate 5 K peak-to-peak variation. At the same time, the measured force varies by approximately 1 mN, although it does not seem to be a result of the ΔT. The random drift of the force measurement is a similar magnitude to this, at approximately 1 $mN.hr^{-1}$. This relative insensitivity of the thrust stand to temperature variation is however lost as soon as the pendulum is locked in place and no longer free to swing. When locked, or preloaded with 180 mN, there is a clear correlation between the temperature and measured force, at about 0.6 $mN.K^{-1}$ (using the temperature reading at location 'C1').

Furthermore the thrust stand is more sensitive to a temperature distribution that is asymmetrical about the pivot axis, as would occur from an off-center heat source. This case is shown in the right column of Fig. 6, panels (c) and (d), where the heater has been

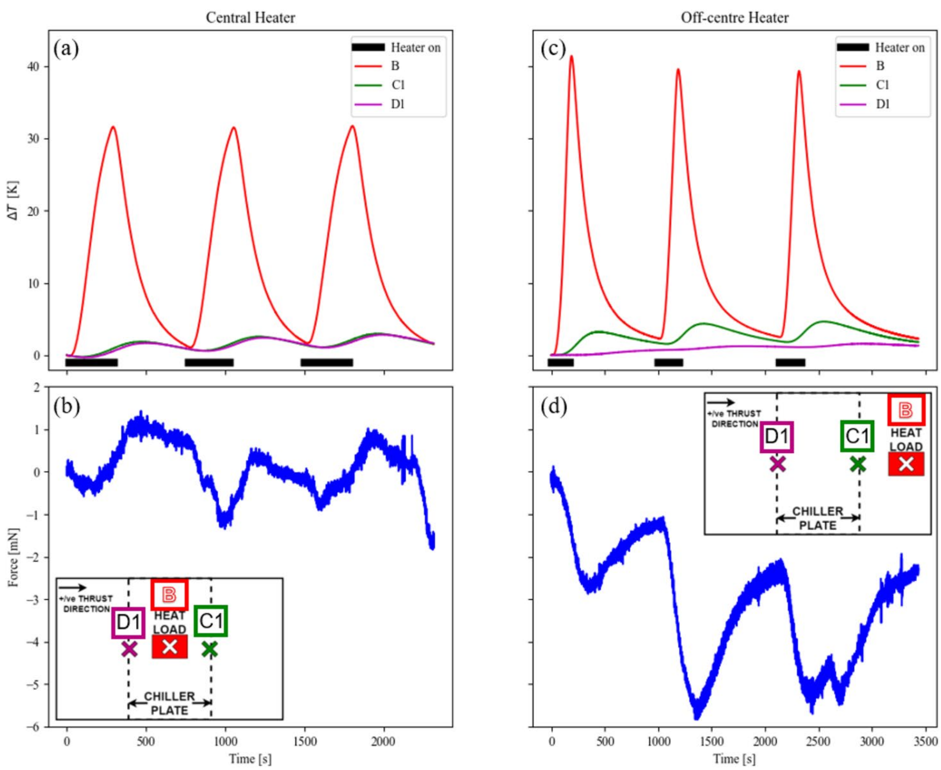

Fig. 6 Temperature sensitivity studies of the thrust stand at Robinson. The first column displays results where the heat source is in the centre of thrust stand, and the second column with an off-centred heat source. Panel **a** shows the temperature change at locations marked by coloured crosses in the schematic in panel **b**; B (on the heater, which is marked as a red rectangle in the schematics), C1 and D1. The heat source is duty cycled as indicated by the bars at the bottom of panels **a** and **c** showing at which times the heater is on. Panels **c** and **d** show the case when heat source is off-centre

moved to the end of the thrust stand. There is now a 5 K difference between the ΔT of 'C1' and 'D1', and a clear correlation between the measured force and the temperature with a peak-to-peak variation between 3 and 5 mN. Our hypothesis is that a thermal expansion of one side of the stand shifts the CoM causing the force.

In the appendix, we further test this hypothesis by undertaking a simplified analysis of the force produced by such an asymmetric temperature distribution. We find;

$$F_z \approx \frac{L_0 Mg}{3l}\alpha(\Delta T_+ - \Delta T_-) \tag{1}$$

where M is the total mass of the pendulum, $2L_0$ is the length of the pendulum plate (in the direction of the thrust measurement) at ambient temperature, α is the linear expansion coefficient in temperature of the pendulum plate, $\Delta T_\pm$ are the difference in temperature over ambient at each end of the plate, and l is the pendulum length. For the experiment shown in Fig. 6c and d we take $\Delta T_+ - \Delta T_- \approx 10$ K, noting that the temperature measurements at 'C1' and 'D1' are not at the ends of the platform, and that the temperature gradient along the length of the thrust stand will not be linear (a simplification made in the derivation of Eq. 1). Combining this with values for the thrust stand at Robinson we calculate a force of 3 mN. Despite its many simplifications, this first-order calculation is remarkably close to the magnitude of the effect measured in experiments which we interpret as supporting our hypothesis as to its origin. A finite-element model and calculation can be used, incorporating this physics, to improve the precision in estimating this form of temperature sensitivity.

Discussion

The experiments described above were undertaken so that direct and accurate thrust measurements of a superconducting AFMPDT can be made at both Robinson and DLR. The results thus far are very promising in light of that goal.

The effect of stray magnetic fields from the magnet we conclude will contribute an uncertainty of less than 1 mN. After some modifications to the measurement hardware, as discussed in the results section, there was essentially no change in the linearity or scale of the force-calibration with up to 100 mT applied locally to magnetically sensitive parts. This suggests that the parasitic force from the final HTS magnet's field can be nulled out during pre-calibration.

The cryocooler caused vibrations up to $\sim 1g$, yet with simple filtering of the raw data we saw an impact of less than 1 mN on the accuracy of our measurements, as indicated by the deviation between the measured force and the calibration weights. Indeed, adding an oscillator to a thrust stand may be a worthwhile strategy to reduce hysteresis arising from stiction.

Temperature variation on the other hand has a significant and non-trivial impact on the thrust. It is not well captured by a mN.K^{-1} metric, since it acts largely by thermal-expansion-induced changes in the CoM and so is sensitive to the specific hardware configuration on the thrust stand and its temperature profile. Nevertheless, we found that if the thermal-induced background drift is confidently known, e.g. a linear drift as seen in the inset to Fig. 5b, the force can be precisely measured to within 1 mN.

As such, we deem it achievable to reduce the measurement inaccuracy of the AFMPDT due to its field, vibrations and waste heat to within ± 3 mN at our facilities, compared with an expected total thrust up to 100 mN (depending on the operating conditions). For example, a full uncertainty analysis of the thrust stand at Robinson, detailed in [10], gave a ± 2.3 mN standard uncertainty using a 5 equal weights producing a 68 mN scale, whilst operating water cooling and a CT cryo-cooler at 140 W and whose heat flux sunk to the thrust stand. Of course, this remains to be demonstrated for the superconducting AFMPDT, especially as the full magnetic field profile and temperature-induced hardware CoM changes could not so far be tested on our thrust stands.

The most significant outstanding consideration and risk to accurate thrust measurements remains thermal management. For example, thermally-induced drift in the baseline force reading could make accurate thrust measurements difficult, requiring significant post-processing of the data and assumptions in the baseline drift to be made. More severely, there is a risk that thermal-induced drift causes the force reading to go out-of-range before the AFMPDT experiment can be completed. This was already seen just after 14:30 in the experiment shown in Fig. 5, albeit under conditions designed to maximize the thrust stand's thermal sensitivity. That risk is exacerbated in our case by the extended length of time ($\sim$1 day) required to have the cryocooler operating in vacuum, and dissipating up to 180 W of heat flux, before the superconducting magnet is at its operational temperature. Furthermore, we believe it an important capability to have the thruster running for several hours whilst still being able to make thrust measurements. A way to mitigate the risk of drifting out-of-range, which has been implemented so far on the Robinson thrust stand, is to operate the displacement sensor at 75% of its maximum linear range, with thrust lowering this value. With this method, a −25% offset can be tolerated, that may be caused by either magnetic or thermal effects.

The experiments in this paper have also informed what further design considerations and optimizations can be made to the measurement systems and the AFMPDT so that accurate thrust data can be obtained. The most important again relate to thermal management; effective cooling of the heat-sources on the thrust stand, temperature monitoring and control of the thrust stand, and using high-thermal conductivity paths for an isotropic temperature distribution about the pivot axis of the thrust stand. Less likely to severely impact thrust measurements, though still worth considering is characterizing and managing potential acoustic resonances between a fully-laden thrust stand and vibration harmonics from the cryocooler. And for completeness, we note there are many other considerations that go into making accurate, direct thrust measurements of EP systems which have been discussed in the literature, see e.g. Refs. [4, 15] and citations therein, which will add uncertainty to our final thrust measurements. Pending a full assessment in the final thruster configuration, we assign here an additional 1 mN contribution so that our total predicted uncertainty for the flight-like superconducting AFMPDT is ± 3 mN.

The key next stage of this project however involves comparative measurements of a superconducting AFMPDT at Robinson and DLR, planned to run throughout 2025. By significantly reducing the size, weight and power of the magnet system, superconducting magnet technology significantly improves the attractiveness of AFMPD electric propulsion. Confidence in the accuracy of performance data from flight-like AFMPDT hardware, especially thrust data, also significantly improves the likelihood of the technology's uptake. As such, we see this project as an important part of taking AFMPDTs out of the laboratory, and into space.

Conclusion

Robinson and DLR are working together on a project to measure thrust from an AFMPDT with a conduction-cooled superconducting magnet used for the applied field module. In this paper we presented results of the characterization and modification of the thrust stands at DLR and Robinson to meet the additional challenges of associated with direct and accurate thrust measurement of such an AFMPDT. We found that after some relatively minor modifications to parts, the stray magnetic field expected from the superconducting magnet will have a negligible impact on the accuracy of our force measurements. The vibrations from a cryocooler on the thrust stand, although large at approximately 1g peak acceleration, can be effectively filtered out in post processing of the data. Moreover, the vibrations may improve the quality of the measurement by reducing hysteresis arising from bearing stiction. A variety of methods will need to be carefully employed to reduce the sensitivity to temperature, particularly to an uneven temperature distribution across the pivot axis. As such, with careful design and characterization work such as that laid out in this paper, we deem it feasible to make direct thrust measurement of a flight-like superconducting AFMPDT accurate to within ±3 mN. We are looking forward to the next phase of this project.

Appendix

Here we present a first-order calculation of the force due to a temperature distribution about the pivot axis on the thrust stand at Robinson. The intent is to check the plausibility of our hypotheses described in the "Thermal effects" section - in particular, that the temperature sensitivity of the thrust stand results in large part from an asymmetric temperature distribution about the pivot axis. As such, we make several simplifying assumptions in pursuit of a tractable analytical expression. Finite-element modelling should be used for more precise calculations.

We start by making the simplification that the thrust platform is perfectly rigid in the two axes perpendicular to the thrust direction, z. The dimension of the platform in that direction changes with temperature according to;

$$\Delta L = L_0 \alpha \Delta T \tag{2}$$

where α is the linear expansion coefficient, which we take as 2.2×10^{-5} K^{-1} for the aluminium of the platform plate. The centre of mass of the platform is;

$$z_{\mathrm{CoM}} = M^{-1} \int_0^M z dm \tag{3}$$

where we are integrating over mass-elements dm at each position z along the length of the platform, up to the total mass of the platform M. Each mass-element is $dm = \lambda dz$, where $\lambda = \rho HW$ is the linear mass density (or, ρ the density with W the width and H the height of the platform). We take the origin of the z-axis to be in the centre of platform and its total initial length to be $2L_0$, and so with the thrust stand isothermal at ambient temperature the expression for the centre of mass becomes;

$$z_{\mathrm{CoM}} = M^{-1} \int_{-L_0}^{L_0} \lambda z dz = 0 \tag{4}$$

To incorporate the effect temperature gradients, we alter the limits of the integration in this expression according to Eq. 2 and use $\Delta T_{\pm}$ to denote the temperature change with respect to the ambient temperature starting point at either end of the platform; that is, at $z = L_0$ and $z = -L_0$ respectively. We also account for a variation in density with temperature which we approximate as $\Delta\lambda = \lambda_0 \epsilon \Delta T$. To determine the coefficient ϵ, we use the conservation of mass of the stand;

$$M = \int_{-L_0}^{L_0} \lambda dz = \int_{-(1+\alpha\Delta T_-)L_0}^{(1+\alpha\Delta T_+)L_0} \lambda \left(1 + \epsilon \Delta T_{(z)}\right) dz \tag{5}$$

A highly simplified expression for the temperature distribution along the thrust stand is;

$$\Delta T_{(z)} = \left(\frac{\Delta T_+ - \Delta T_-}{2L_0}\right)z + \frac{1}{2}(\Delta T_+ + \Delta T_-) \tag{6}$$

A more accurate temperature distribution will be non-linear, and in the specific case of the experiment in Fig. 6 would account for the the chiller plate in the central third of the thrust stand regulating the temperature. These improvements to the calculation are best implemented numerically with finite element modelling. For the analytical treatment here, we use this linear expression for the temperature distribution to solve Eq. 5 and find, after some algebra, that;

$$\epsilon \approx -\alpha \tag{7}$$

where we have used $\alpha\Delta T_\pm \ll 1$ to simplify the result.

Bringing together then Eqs. 4, 6 and 7 the expression for the centre of mass with our asymmetric temperature distribution becomes;

$$\begin{aligned} z_{\text{CoM}} &= M^{-1}\int_{-(1+\alpha\Delta T_-)L_0}^{(1+\alpha\Delta T_+)L_0} \lambda\left[1-\alpha\left[\left(\frac{\Delta T_+ - \Delta T_-}{2L_0}\right)z + \frac{1}{2}(\Delta T_+ + \Delta T_-)\right]\right]zdz \\ &\approx (\lambda 2L_0)^{-1}(2/3)\lambda L_0^2\alpha(\Delta T_+ - \Delta T_-) \\ &= \frac{\alpha}{3}(\Delta T_+ - \Delta T_-)L_0 \end{aligned} \tag{8}$$

where we have neglected terms with α^2. If the temperature distribution about the centre of the platform (the pivot plane) is symmetric, then $\Delta T_+ = \Delta T_-$ and there is no change in the centre of mass. This is not the case for the experiments shown in Fig. 6c and d, where $\Delta T_+ - \Delta T_- \approx 10$ K (noting that $\Delta T_\pm$ refer to the temperatures at the ends of the thrust stand, whereas our temperature measurements at positions 'C1' and 'D1' are about 1/3 of the way in from the ends). By using Eq. 8 and the length of our stand $2L_0 = 0.45$ m, we estimate that that asymmetric temperature distribution leads to a shift in the centre of mass of approximately 17 μm.

The angular deflection, θ, of the thrust stand due to the small change in the centre of mass from zero is;

$$\sin\theta = \frac{z_{\text{CoM}}}{l} \tag{9}$$

where the pendulum arm length of the thrust stand at Robinson is $l = 0.525$ m. That leads to a component of force in the thrust-direction, z, of;

$$\begin{aligned} F_z &= Mg\tan\theta \\ &\approx \frac{Mgz_{\text{CoM}}}{l} \end{aligned} \tag{10}$$

where the small-angle approximation used in the second line is a good approximation. The mass of the platform during the experiments shown in Fig. 6 was 10 kg, and so we arrive at a first-order estimate of the force due to a 10 K asymmetric temperature distribution to be 3 mN. This value is remarkably close to that measured, see Fig. 6d, despite the various simplifications we have made in the analysis presented above. We take the agreement between the calculation and experiments to support the plausibility of our hypothesis that an asymmetric temperature distribution about the pivot axis is the major cause of temperature sensitivity in our thrust measurements.

Acknowledgements
We thank Dr. Stuart Wimbush and Dr. Andreas Hermann for their early input into this collaboration.

Authors' contributions
All authors contributed equally to the manuscript.

Funding
This work was funded by the New Zealand Ministry of Business, Innovation and Employment through the project "Thrust Measurement of Small-scale Electric Propulsion Systems Incorporating Cryogenic Technologies and High Magnetic Fields", contract number RTVU2111.

Data availability
Data available on request.

Declarations

Competing interests
The authors declare no competing interests.

Received: 25 September 2024 Accepted: 25 January 2025
Published online: 13 February 2025

References

1. Coogan W, Choueiri E (2017) A critical review of thrust models for applied-field magnetoplasmadynamic thrusters. In: 53rd AIAA/SAE/ASEE Joint Propulsion Conference AIAA Propulsion and Energy Forum, American Institute of Aeronautics and Astronautics. https://arc.aiaa.org/doi/10.2514/6.2017-4723
2. Balkenhohl J, Glowacki J, Rattenbury N, Cater J (2023) J Electr Propuls 2:1. ISSN 2731–4596. https://doi.org/10.1007/s44205-022-00036-5
3. Acheson C, Glowacki J, Nakano R, Maeshima D, Saile D, Pavri B, Takagi R, Mori R, Pollock R, Olatunji J, Goddard-Winchester M, Strickland N, Ichihara D, Wimbush S, Kinefuchi K (2023) J Electr Propuls 2:26. ISSN 2731–4596. https://doi.org/10.1007/s44205-023-00060-z
4. Polk JE, Pancotti A, Haag T, King S, Walker M, Blakely J, Ziemer J (2017) J Propuls Power 33:539–555. American Institute of Aeronautics and Astronautics. https://arc.aiaa.org/doi/10.2514/1.B35564
5. Voronov AS, Troitskiy AA, Egorov ID, Samoilenkov SV, Vavilov AP (2020) J Phys Conf Ser 1686:012023. ISSN 1742-6596. Publisher: IOP Publishing. https://doi.org/10.1088/1742-6596/1686/1/012023
6. Zheng J, Liu H, Song Y, Zhou C, Li Y, Li M, Tang H, Wang G, Cong Y, Wang B, Wang Y, Wu P, Qu T, Zhu X, Zhu L, Liu F, Cheng Y, Zhao B (2021) Sci Rep 11:20706. ISSN 2045-2322. bandiera_abtest: a Cc_license_type: cc_by Cg_type: Nature Research Journals Number: 1 Primary_atype: Research Publisher: Nature Publishing Group Subject_term: Engineering;Physics;Space physics Subject_term_id: engineering;physics;space-physics. https://www.nature.com/articles/s41598-021-00308-4
7. Long N, Rao A, Olatunji J, Badcock R, Balkenhohl J, Berry T, Cater J, Glowacki J, Goddard-Winchester M, Hann CE, Harris P, Limmer-Wood A, Mallett BPP, Rattenbury N, Strickland N, Weaver T, Webster E, Weijers HW, Wimbush S, Wright D (2022) Toward On-Orbit Demonstration of a High Temperature Superconducting AF-MPD Thruster, Electric Rocket Propulsion Society, Boston, p 480. https://www.electricrocket.org/IEPC_2022_Papers.html
8. Pollock R, Głowacki J, Goddard-Winchester M, Hellmann S, Huang X, Mallett B, Olatunji J, Pavri B, Shellard C, Strickland N, Webster E, Rao A, Wright D, Parashar T (2024). In: 2024 IEEE Aerospace Conference, Big Sky, MT, USA, pp 1–11. https://doi.org/10.1109/aero58975.2024.10521198
9. Glowacki J, Webster E, Hellmann S, Smart S, Sidorov G (2024) Discharge characteristics of a low-power applied-field magnetoplasmadynamic thruster in a tesla-level magnetic field. Electric Rocket Propulsion Society, Toulouse
10. Webster E, Mallett B, Jane C, Smart S (2024). In preparation
11. Neumann A (2018) J Large-Scale Res Facil 4:A134–A134. ISSN 2364-091X. https://jlsrf.org/index.php/lsf/article/view/169
12. Neumann A, Simon J, Schmidt J (2021) EPJ Tech Instrum 8:1–19. ISSN 2195-7045. Number: 1. Publisher: SpringerOpen. https://epjtechniquesandinstrumentation.springeropen.com/articles/10.1140/epjti/s40485-021-00074-7
13. Schmidt J, Simon J, Neumann A (2023) Int J Energetic Mater Chem Propuls 22. ISSN 2150-766X. 2150-7678. Publisher: Begel House Inc. https://www.dl.begellhouse.com/journals/17bbb47e377ce023,7b1719907bb1c9ee,72deb2bf1deda939.html
14. Haag TW (1991) Rev Sci Instrum 62:1186–1191. ISSN 0034-6748. Publisher: American Institute of Physics. https://aip.scitation.org/doi/abs/10.1063/1.1141998
15. Neumann A, Volkmar C, Geile C, Hannemann K (2017) Mitigation of detrimental electric thruster force measurement effects. In: 35th International Electric Propulsion Conference, Georgia Institute of Technology, Electric Rocket Propulsion Society. https://elib.dlr.de/115125/